



ELSEVIER

BOLETIN DE LA SOCIEDAD ESPAÑOLA DE

Cerámica y Vidrio

www.elsevier.es/bsecv



## Synthesis of pigments of $\text{Fe}_2\text{O}_3 \cdot \text{SiO}_2$ system, with Ca, Mg, or Co oxide additions

Tsvetan Dimitrov<sup>a</sup>, Stephan Kozhukharov<sup>b,\*</sup>, Nikolay Velinov<sup>c</sup>

<sup>a</sup> “Angel Kanchev” University of Ruse – Branch Razgrad, 47 “Aprilsko vastanie” blvd., 7200 Razgrad, Bulgaria

<sup>b</sup> University of Chemical Technology and Metallurgy, 8 “Klyment Okhridsky” blvd., 1756 Sofia, Bulgaria

<sup>c</sup> Institute of Catalysis, Bulgarian Academy of Sciences, Acad. “Gerorgy Bonchev” blvd., Block 11, 1113 Sofia, Bulgaria

### ARTICLE INFO

#### Article history:

Received 28 July 2016

Accepted 10 November 2016

Available online xxx

#### Keywords:

Pigments

Dopants

X-ray Diffraction spectroscopy

Electron Paramagnetic Resonance

Mössbauer spectroscopy

Scanning Electron Microscopy

Energy Dispersion X-ray

spectroscopy

### ABSTRACT

The present research work is based on the comparative evaluation of the Ca, Mg, and Co dopant impact on the properties of new ceramic pigments from the system  $\text{Fe}_2\text{O}_3 \cdot \text{SiO}_2$  obtained via classical ceramic technology. This approach enabled determination of the optimal temperature for the synthesis and the most appropriate mineralizer. The obtained specimens were submitted to systematical analysis, including X-ray Diffraction (XRD) spectroscopy, Electron Paramagnetic Resonance (EPR) analysis and Mössbauer spectroscopy for crystalline phase determination. The color characteristics are quantified by spectrophotometric measurements. The pigments particle size has been determined by Scanning Electron Microscopy (SEM), combined by Energy Dispersion X-ray spectroscopy (EDX). The obtained results enabled to determine the correlation between the calcination temperature and the phase compositions of the obtained pigments. In addition, some interesting magnetic properties were detected for the Co-doped composition.

© 2016 SECV. Published by Elsevier España, S.L.U. This is an open access article under the CC BY-NC-ND license (<http://creativecommons.org/licenses/by-nc-nd/4.0/>).

### Síntesis de pigmentos del sistema $\text{Fe}_2\text{O}_3 \cdot \text{SiO}_2$ con adiciones de óxidos de Ca, Mg o Co

### RESUMEN

La investigación presente está basada en la evaluación comparativa del efecto de la adición de los óxidos de Ca, Mg, y Co sobre las propiedades de unos pigmentos cerámicos nuevos del sistema  $\text{Fe}_2\text{O}_3 \cdot \text{SiO}_2$  obtenidos mediante la tecnología cerámica clásica. Ese método de investigación ha permitido la determinación de la temperatura de calcinación óptima y el mineralizador más apropiado. Las muestras obtenidas fueron sometidas al análisis sistemático, incluyendo espectroscopia de difracción de rayos X, análisis de la resonancia electrónica paramagnética (REP) y espectroscopia de Mössbauer para la determinación de las fases cristalinas constituyentes. Los parámetros colorimétricos han sido evaluados mediante medidas espectrofotométricas. El tamaño estimado de las partículas se ha

#### Palabras clave:

Pigmentos

Dopantes

Espectroscopia de difracción de rayos X

Resonancia electrónica

paramagnética

Espectroscopia de Mössbauer

Microscopia electrónica de barrido

Dispersión energética de rayos X

\* Corresponding author.

E-mail address: [stephko1980@abv.bg](mailto:stephko1980@abv.bg) (S. Kozhukharov).

<http://dx.doi.org/10.1016/j.bsecv.2016.11.001>

0366-3175/© 2016 SECV. Published by Elsevier España, S.L.U. This is an open access article under the CC BY-NC-ND license (<http://creativecommons.org/licenses/by-nc-nd/4.0/>).

determinado por microscopia electrónica de barrido (MEB) y su composición elemental se ha definido mediante la espectroscopia de dispersión energética de los rayos X (EDEX). Los resultados obtenidos han permitido la determinación la correlación entre la temperatura de calcinación y las composiciones cristalinas de los pigmentos obtenidos. En adición, se han registrado algunas propiedades magnéticas interesantes en el caso de la composición dopada por cobalto.

© 2016 SECV. Publicado por Elsevier España, S.L.U. Este es un artículo Open Access bajo la licencia CC BY-NC-ND (<http://creativecommons.org/licenses/by-nc-nd/4.0/>).

## Introduction

The ceramic pigments are important class materials which determine the color related characteristics, as well as other properties of the obtained ceramic products. Besides, the pigment addition enables enhancement of the resistance against atmospheric, thermal and chemical impact of the surrounding environments, especially the decomposing impact of silicate fusions (e.g. frits) and sun-light related UV-photochemical decomposition. These colored inorganic compounds should possess a high light refraction coefficient, and to be insoluble in water, organic solvents, ceramic slips, in order to form stable colloidal precursor systems with desirable color related characteristics [1].

The color possessed by a given pigment appears as a result of the selective light wave absorption by its crystalline lattice at defined wavelength. The color of given pigment is being determined by the presence of chromophores. They are composed by atoms or atomic groups capable to render colorization of the respective ceramic system containing them [2].

The color related characteristics are always derived by chemical compounds of d- or f-transition elements, such as vanadium, iron, cobalt, manganese, nickel, copper, chromium, praseodymium, etc.

Following their specific function, the pigments can be concerned as an entire class of materials. These compounds can be grouped by different indications. One of the most versatile and widely classifications used is drawn up by the Color Pigments Manufactures Association (CPMA) formerly the Dry Color Manufactures Association (DCMA) in the United States. This system provides a structural classification of pigments on the basis of the main substance crystalline lattice type. According to this classification, the pigments are divided into: spinel, garnet, zircon, olivine, baddeleyite, periclase, etc. [3,4].

Although the zircon-based pigments are relatively new class, they are already among the most perspective and widely used in the industrial practice, because of their remarkable thermal stability in glaze melts. The most distinguishable representatives of the Zr-based pigments are: vanadium zircon blue [5–8], praseodymium zircon yellow [5,9,10], iron-zircon pink [11–16], etc.

Other group of interesting high temperature resistant emerald-green pigments is developed on the basis of the mineral uvarovite. These pigments can be obtained from natural precursors at high temperatures (1200–1250 °C) at the presence of mineralizers (mainly borates and fluorides), and

currently the processes involved in their synthesis are object of intensive scientific research activities [14–16].

The pigments based on spinel compounds also possess high color intensity, chemical and thermal stability. The structural and crystalline lattice similarity among various spinel based pigments enables isomorphic substitution with solid solution formation. Examples for stable pigments from this group are elaborated on the basis of  $\text{CaFe}_2\text{O}_4$  [17],  $\text{MgFe}_2\text{O}_4$  [18],  $\text{CoFe}_2\text{O}_4$  [19–23], etc.

The aim of the present research work is to synthesize, and characterize doped ceramic pigments on the basis of  $3\text{MeO}\cdot\text{Fe}_2\text{O}_3\cdot\text{SiO}_2$ , where “Me” is Ca, Mg, or Co.

## Experimental

### Sample preparation

#### Initial precursors

Three compositions were investigated in the present research work:  $3\text{CaO}\cdot\text{Fe}_2\text{O}_3\cdot 3\text{SiO}_2$  (composition 1),  $3\text{MgO}\cdot\text{Fe}_2\text{O}_3\cdot\text{SiO}_2$  (composition 2) and  $3\text{CoO}\cdot\text{Fe}_2\text{O}_3\cdot\text{SiO}_2$  (composition 3). These compositions were selected on the basis of literature analysis, and preliminary experiments, as well as considering that the color should be originated from the following chromophores:  $\text{Ca}_3\text{Fe}_2\text{Si}_3\text{O}_{12}$ ,  $\text{MgFe}_2\text{O}_4$ , and  $\text{CoFe}_2\text{O}_4$ . Following the literature,  $\text{H}_3\text{BO}_3$  was added in quantities relevant to 2%<sub>wt.</sub> of the entire pigment composition, in order to act as a mineralizer [24–28]. The precursors used for pigment synthesis were, as follows: CaO, (Reachim) MgO, (Reachim) CoO (Sigma–Aldrich),  $\text{Fe}_2\text{O}_3$  (Sigma–Aldrich),  $\text{SiO}_2\cdot n\text{H}_2\text{O}$  and  $\text{H}_3\text{BO}_3$  (Reachim). All these precursors were with analytical grade of purity.

The hydrated  $\text{SiO}_2\cdot n\text{H}_2\text{O}$ , used in the present case is much more reactive than the pure quartz sand and has particle size dimensions between 2 and 7  $\mu\text{m}$ . Initially, after calcination in a platinum crucible, its composition was estimated to 76.3% of  $\text{SiO}_2$  and 23.7% of  $\text{H}_2\text{O}$  (i.e. 4:1), respectively.

#### Pigment synthesis

The necessary precursor quantities for 100 g precursor mixture were weighted by a balance with  $\pm 0.1$  g of precision, and subsequently dry ball-milled in PULVERIZETE – 6 product of “FRITCH” (Germany).

The pigment synthesis was performed in a muffle furnace by heating speed – 300–400 °C/h at air atmosphere in covered crucibles and isothermal step continuation for 2 h at 800 °C, 900 °C, 1000 °C, 1100 °C and 1200 °C, respectively. The technological schedule scheme is represented in Fig. 1.

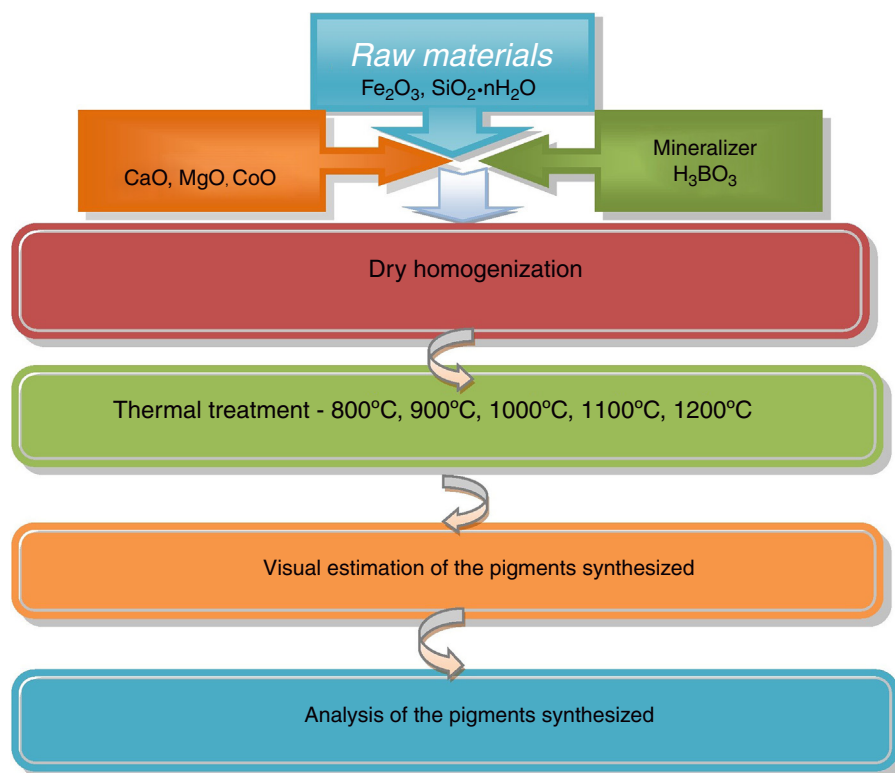


Fig. 1 – Pigment synthesis technological schedule scheme.

#### Glaze deposition

Some of the pigments were deposited in semi-industrial conditions, in “KAI Group-Khan Asparuh-JSC”-Bulgaria, on biscuit ceramic plates. The glaze mixtures were composed by 5%<sub>wt.</sub> pigment addition, in basic frit with supplemental 7%<sub>wt.</sub> kaolin content. The composition of the basic frit is shown in Table 1.

The obtained mixtures were submitted in ball milling by “PULVERIZETE – 6” for 30 min prior to use. The subsequent glazing was performed by pouring of the above described glazes on biscuit tile plates with 16% of water uptake capability. Afterwards, the samples were submitted to thermal treatment in rolling furnace for 40 min at 1145 °C.

#### Sample characterization techniques

##### The X-ray Diffraction (XRD)

This analysis was performed by IRIS X-ray analyzer with Cu K<sub>α</sub> cathode and Ni filter in interval from 10° to 60° and powered at 40 kV × 40 mA. Diffractograms were registered for 2θ values, with an increasing step of 0.02° each 3 s.

##### The Electron Paramagnetic Resonance (EPR)

The spectra were acquired by BRUKER EMX PREMIUM X, with temperature conditioner – ER4141-VT UNIT in temperature range from 120 to 450 K.

##### Mössbauer spectroscopy

The Mössbauer spectra were obtained in air at room temperature (RT) with a Wissenschaftliche Elektronik GmbH, electromechanical spectrometer working in a constant acceleration mode. A <sup>57</sup>Co/Rh (activity ≅ 50 mCi) source and α-Fe

standard were used. The experimentally obtained spectra were fitted using CONFIT2000 software [15]. The parameters of hyperfine interaction such as isomer shift (δ), quadrupole splitting (Δ), effective internal magnetic field (B), line widths (Γ<sub>exp</sub>), and relative weight (G) of the partial components in the spectra were determined.

##### SEM/EDX observations

The particle morphologies of the investigated pigments were submitted to Scanning Electron Microscopy, performed by TESCAN, SEM/FIB LYRA I XMU at 1500 folds of magnifications. The SEM observations were combined by Energy Dispersion X-ray (EDX) analysis done by “Quantax-8” detector.

##### Colorimetry

The pigment color characteristics were quantified by Lovibont Tintometer RT 100. This measurement procedure was applied for the obtained tiles, as well.

## Results and discussion

### XRD analysis results

The acquired X-ray patterns of the obtained pigments are shown in Figs. 2–4.

The 3CaO·Fe<sub>2</sub>O<sub>3</sub>·3SiO<sub>2</sub> pigments, calcined at 900 °C showed indicative reflections for andradite, and their intensity increased with the calcination temperature elevation. This increase coincided with intensity decrement of the rest picks, corresponding to wollastonite, hematite and

**Table 1 – Nominal metal oxide content of the basic frit.**

Metallic oxide	SiO <sub>2</sub>	Al <sub>2</sub> O <sub>3</sub>	Fe <sub>2</sub> O <sub>3</sub>	CaO	Na <sub>2</sub> O	ZrO <sub>2</sub>	BaO	B <sub>2</sub> O <sub>3</sub>	K <sub>2</sub> O	ZnO	MgO
Content % <sub>w.t.</sub>	57.94	5.52	0.20	3.43	6.25	9.08	2.15	13.33	0.25	0.98	0.14

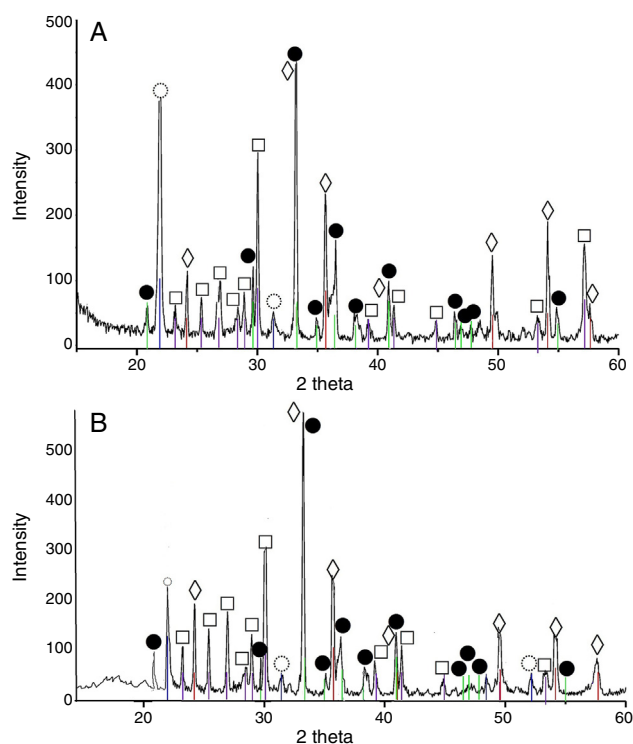


**Fig. 2 – X-ray patterns of the 3CaO·Fe<sub>2</sub>O<sub>3</sub>·3SiO<sub>2</sub> system sintered at 1000 °C (A) and 1100 °C (B). ● – Andradite Ca<sub>3</sub>Fe<sub>2</sub>Si<sub>3</sub>O<sub>12</sub> – 79 – 1659; □ – Wollastonite CaSiO<sub>3</sub> – 84 – 0654; ◇ – Hematite Fe<sub>2</sub>O<sub>3</sub> – 89 – 0599; ○ – Cristobalite low SiO<sub>2</sub> – 76 – 0941.**

cristobalite. Finally, when the calcination temperature reached 1200 °C an appearance of amorphous phase was observed.

The 3MgO·Fe<sub>2</sub>O<sub>3</sub>·SiO<sub>2</sub> pigment, treated at 900 °C has revealed the occurrence of forsterite, magnesioferrite, hematite and cristobalite. The phase composition altered with calcination temperature in this case, as well by increase of the peak intensity for the former two phases (i.e. magnesioferrite, forsterite).

The pigments from the 3CoO·Fe<sub>2</sub>O<sub>3</sub>·SiO<sub>2</sub> system calcined at 900 °C contained Co<sub>2</sub>SiO<sub>4</sub>, CoFe<sub>2</sub>O<sub>4</sub> and cristobalite. The calcination temperature elevation caused increase of the CoFe<sub>2</sub>O<sub>4</sub> peak intensity increment.

#### Electron Paramagnetic Resonance analysis

The EPR spectrum of composition 2, recorded at 450 K is composed by unique, almost symmetric signal with  $g = 2.242$  and  $\Delta H_{pp} \approx 88$  mT (Fig. 5). The analysis temperature lowering caused sharp alterations in the EPR spectra shapes and positions toward the weaker magnetic fields, with simultaneous increase of peak width and anisotropy. The EPR signal shape

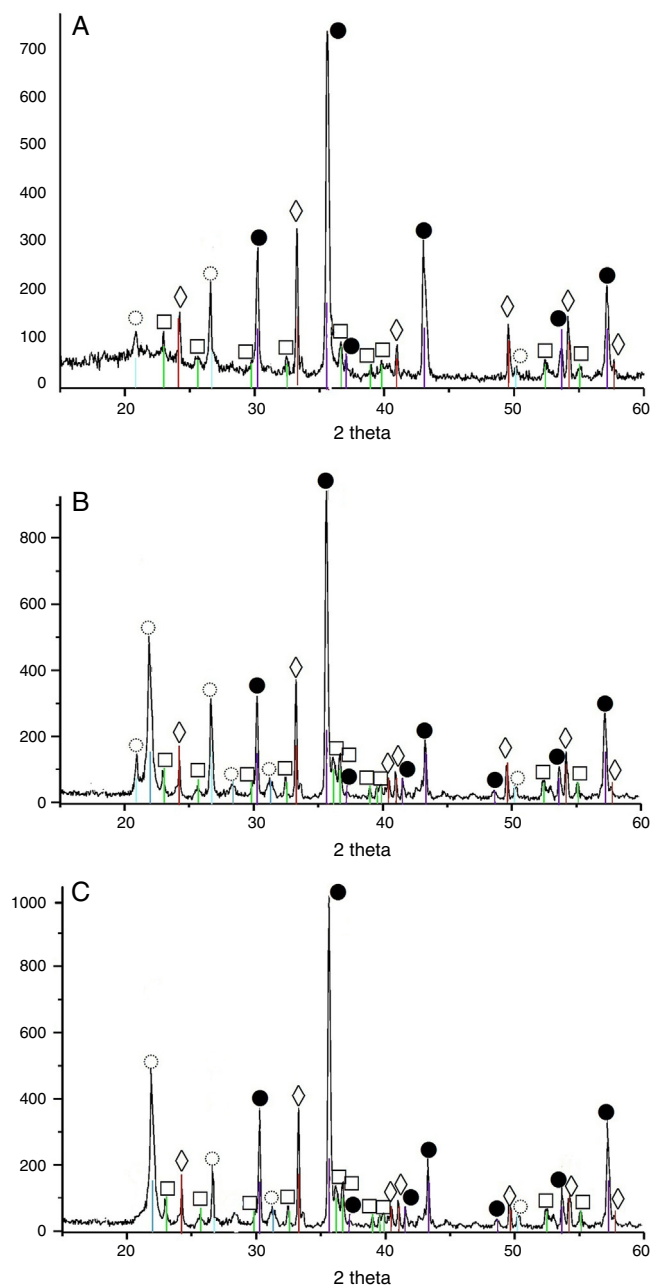


**Fig. 3 – X-ray patterns of the 3MgO·Fe<sub>2</sub>O<sub>3</sub>·SiO<sub>2</sub> sintered at 1000 °C (A), 1100 °C (B) and 1200 °C (C). ● – Magnesioferrite MgFe<sub>2</sub>O<sub>4</sub> – 89 – 3084; □ – Forsterite Mg<sub>2</sub>SiO<sub>4</sub> – 85 – 1361; ◇ – Hematite Fe<sub>2</sub>O<sub>3</sub> – 89 – 0599; ○ – Cristobalite SiO<sub>2</sub> – 89 – 3434.**

temperature dependence observed for composition 2 in the 120–450 K range is an indicative for presence of supermagnetic particles. Thus, the EPR signal registered can be attributed to occurrence of Fe<sub>2</sub>O<sub>3</sub> in supermagnetic state.

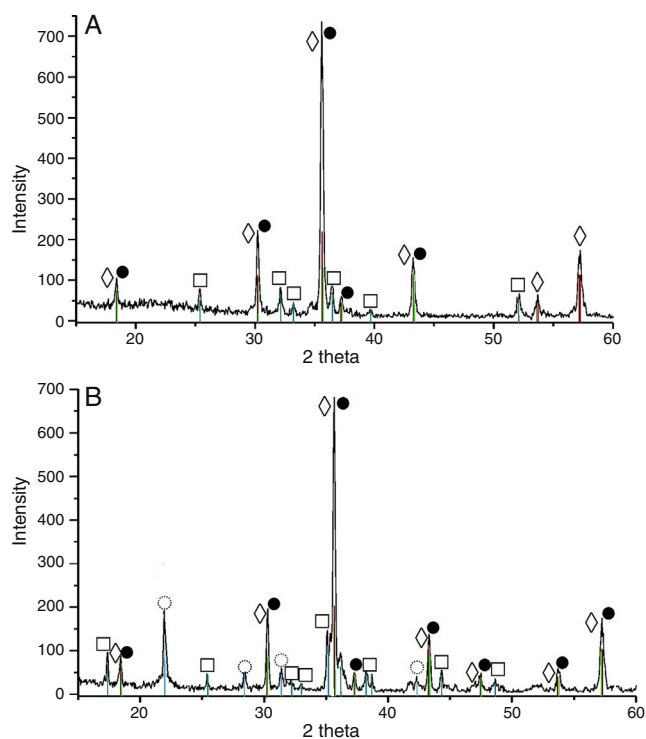


**Fig. 4 – X-ray patterns of the  $3\text{CoO}\cdot\text{Fe}_2\text{O}_3\cdot\text{SiO}_2$  sintered at 900 °C (A) and 1100 °C (B). ● – Cobalt ferrite  $\text{CoFe}_2\text{O}_4$  – 79 – 1744; □ – Cobalt(II) Orthosilicate  $\text{Co}_2\text{SiO}_4$  – 15 – 0865; ◇ – Magnetite  $\text{Fe}_3\text{O}_4$  – 89 – 3854; ○ – Cristobalite  $\text{SiO}_2$  – 89 – 3434.**

The temperature correlation of the EPR signal width and shift for composition 2, shown in Fig. 6 follows the equation for super-paramagnetic state  $H_{pp}^3 = F(H_o(450\text{K}) - H_x)$ . This fact is an evidence for the compositional and size distribution homogeneity of the nano-domains in the powder probe.

The EPR spectrum recorded for composition 3 at 295 K (Fig. 7.) has very wide signal with  $\Delta H_{pp} > 500\text{mT}$ . The analysis temperature elevation until 450K causes simultaneous

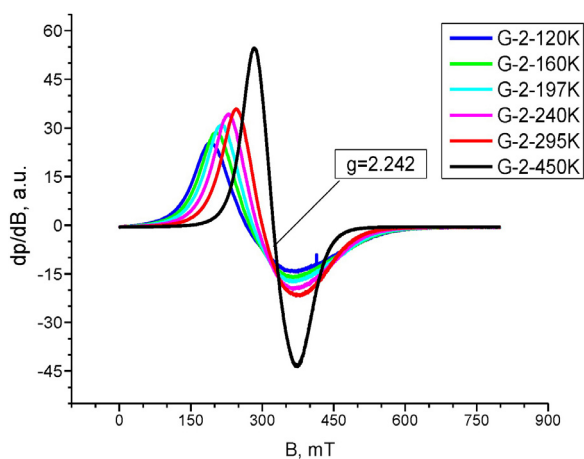


**Fig. 5 – EPR spectrum of pigment from composition 2 sintered at 1100 °C, recorded at 120, 160, 200, 240, 295 and 450 K (the  $g$ -factor describes the signal acquired at 450 K).**

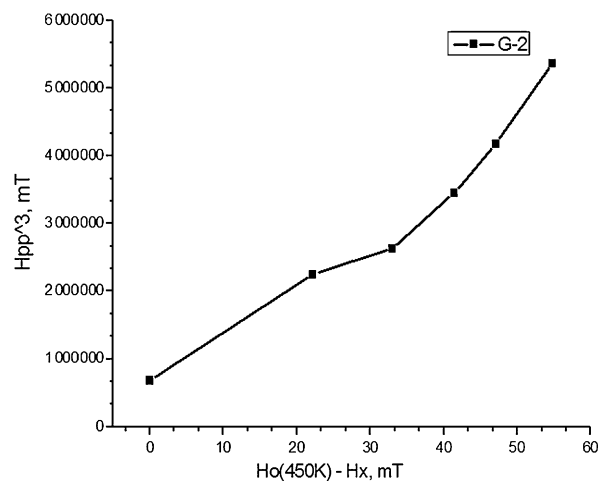
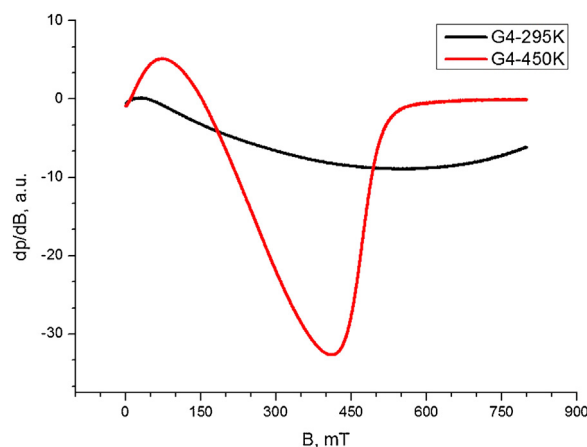


**Fig. 6 – Dependence between the EPR signal band width for composition 2 sintered at 1100 °C, and its positional shift toward weaker magnetic fields.**

narrowing and intensity increase of this signal. The temperature dependence of the EPR signal shape for this composition reveal magnetic exchange interactions between the  $\text{Co}^{2+}$  and  $\text{Fe}^{3+}$  ions. From the spectrum registered at 450K it can be inferred that even at high temperatures, the magnetic bulk interactions remain dominant, whereas the shape of the spectrum acquired 295 K is an indication for magnetically ordered state.

#### Mössbauer spectral analysis of the obtained pigments

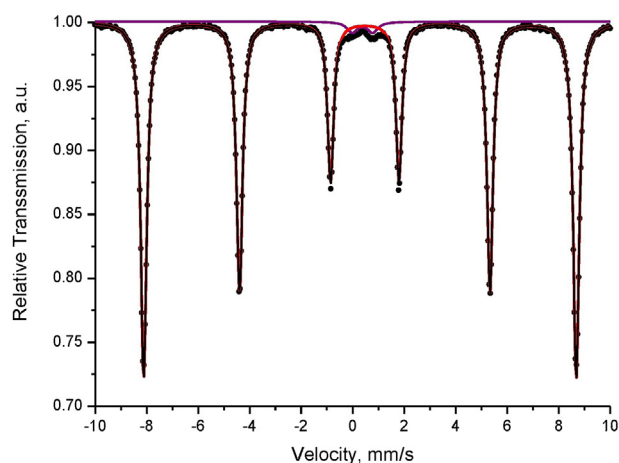
The Mössbauer spectra acquired were consisted either only by doublets or by their combinations with sextets. The most distinguishable spectra of compositions 1 and 2 calcination at 1100 °C were composed by one sextet and one doublet for composition 1 and three sextets combined by one doublet for composition 2, respectively. These spectra are depicted in Figs. 8 and 9, and the corresponding numerical results are summarized in Table 2.



**Fig. 7 – EPR spectrum for composition 3 registered at 295 K and 450 K.**

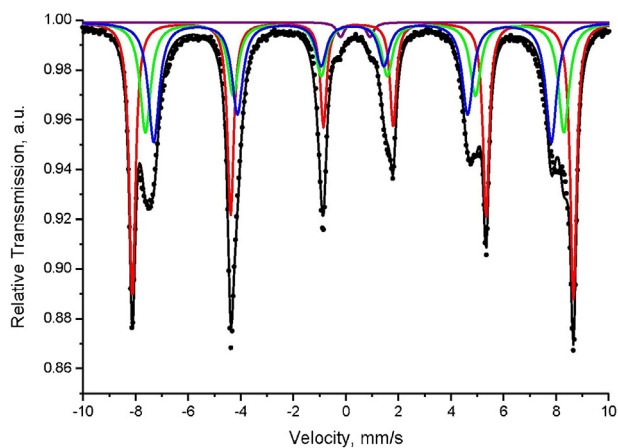
**Table 2 – Mössbauer parameters of the investigated specimens.**

Sample	Components	$\delta$ , mm/s	$\Delta$ , mm/s	B, T	$\Gamma_{\text{exp}}$ , mm/s	G, %
Composition 1 1100 °C (3CaO·Fe <sub>2</sub> O <sub>3</sub> ·3SiO <sub>2</sub> )	Sx1-Fe <sup>3+</sup> <sub>octa</sub> , $\alpha$ -Fe <sub>2</sub> O <sub>3</sub>	0.38	-0.19	52.2	0.29	98
	Db-Fe <sup>3+</sup>	0.38	0.80	-	0.48	2
Composition 2 1100 °C (3MgO·Fe <sub>2</sub> O <sub>3</sub> ·SiO <sub>2</sub> )	Sx1-Fe <sup>3+</sup> <sub>octa</sub> , $\alpha$ -Fe <sub>2</sub> O <sub>3</sub>	0.37	-0.21	52.1	0.29	40
	Sx2-Fe <sup>3+</sup> <sub>octa</sub> , MgFe <sub>2</sub> O <sub>4</sub>	0.33	0.01	49.5	0.49	28
	Sx3-Fe <sup>3+</sup> <sub>tetra</sub> , MgFe <sub>2</sub> O <sub>4</sub>	0.26	0.00	47.0	0.49	31
	Db-Fe <sup>3+</sup> , Fe-silicate	0.36	1.12	-	0.34	1

**Fig. 8 – Mössbauer spectrum registered for composition 1 (i.e. 3CaO·Fe<sub>2</sub>O<sub>3</sub>·3SiO<sub>2</sub>) sintered at 1100 °C.**

The sextet component of composition 1 is related to iron in hematite, whereas the doublet component with relative weight 2% probably corresponds to iron involved in paramagnetic crystalline or amorphous phases.

The Mössbauer spectrum of the sample 2 (Fig. 9) is superposition of three sextets and one doublet. The first sextet (Sx1) has parameters typical for hematite ( $\alpha$ -Fe<sub>2</sub>O<sub>3</sub>), and its relative weight is calculated of 35%. The second and third sextets have isomer shifts typical for iron in third oxidation state in octahedral and tetrahedral coordination, respectively. This is

**Fig. 9 – Mössbauer spectrum registered for composition 2 (i.e. 3MgO·Fe<sub>2</sub>O<sub>3</sub>·SiO<sub>2</sub>) sintered at 1100 °C.**

accordance with XRD analysis where the phase of MgFe<sub>2</sub>O<sub>4</sub> was detected. Moreover, almost equal relative weight of Sx2 and Sx3 and low values of quadrupole splitting prove additionally that these sextets are contribution of inversed cubic ferrite spinel. The low intensive doublet in Mössbauer spectrum has parameters of iron in silicate paramagnetic phases and probably it is contribution of amorphous silicate glass in the sample.

#### Colorimetric measurements

The color is the most important characteristic feature of whatever pigment. It is directly related to all the structural and compositional features owed by the respective pigments. The CIE-L-a-b system serves for quantification of the color related characteristics of various classes of materials and industrial products due to its remarkable versatility, enabling its almost universal application [29,30].

This system is composed by three numerical coordinates:

- $L^*$  – luminosity (or brightness), from black  $L^*=0$  to  $L^*=100$  – white color.
- $a^*$  – green/red scale, with greenish component corresponding to negative values, and reddish component attributed to positive values, respectively.
- $b^*$  – blue/yellow scale, with negative blue segment, and positive yellow segment. Thus, the colorimetric spatial coordinates of CIE-L-a-b system are depicted in Fig. 10.

The color characteristics of the investigated pigments calcined at 1000 and 1100 °C were quantified, using both the former RGB, and the described above CIE-L-a-b systems, and the results are summarized in Table 3.

The data summarized in Table 3 indicate that the calcination temperature elevation results in decrease of the color parameter values toward to darker colors. The highest green segment value/-  $a^*$ /belongs to the pigment of composition 3, (i.e. 3CoO·Fe<sub>2</sub>O<sub>3</sub>·3SiO<sub>2</sub>) calined at 1100 °C.

#### SEM-EDX observations

The SEM images acquired for all the compositions calcined at 1100 °C show coarse particles with size dimensions of about 10–20  $\mu\text{m}$ , accompanied by shapeless smaller particles (Fig. 11).

The coarse shape of the larger particles is a supplemental evidence for the high level of crystallinity of the obtained pigments. The additional shapeless particles probably possess amorphous structures.

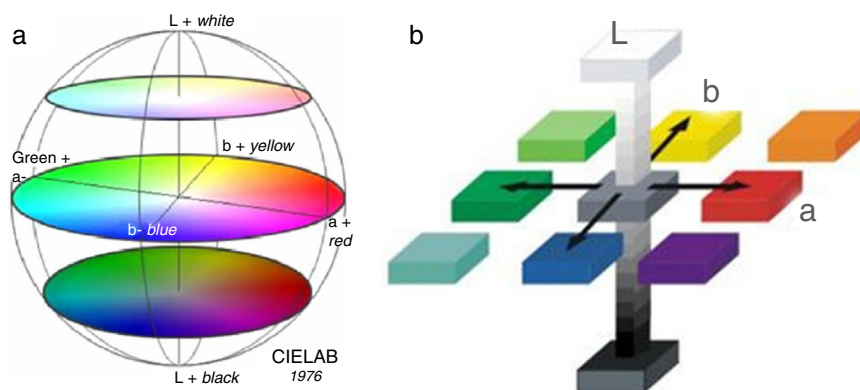


Fig. 10 – Spherical (a) and cubic (b) colorimetric diagrams according to CIE-L-a-b [29,30].

Table 3 – CIE-L-a-b colorimetric parameter values measured for the investigated samples.

Pigment composition	Color	R	G	B	L*	a*	b*
3CaO.Fe <sub>2</sub> O <sub>3</sub> .3SiO <sub>2</sub> Composition 1 1000 °C		106.6	97.6	89.4	41.8	1.8	5.6
3CaO.Fe <sub>2</sub> O <sub>3</sub> .3SiO <sub>2</sub> Composition 1 1100 °C		120.4	109.0	106.5	47.1	4.3	3.2
3MgO.Fe <sub>2</sub> O <sub>3</sub> .SiO <sub>2</sub> Composition 2 1000 °C		218.0	151.4	93.9	67.8	19.2	39.8
3MgO.Fe <sub>2</sub> O <sub>3</sub> .SiO <sub>2</sub> Composition 2 1100 °C		195.6	129.3	85.5	60.2	21.0	34.0
3CoO.Fe <sub>2</sub> O <sub>3</sub> .SiO <sub>2</sub> Composition 3 900 °C		72.7	73.3	69.8	30.6	-1.2	2.2
3CoO.Fe <sub>2</sub> O <sub>3</sub> .SiO <sub>2</sub> Composition 3 1000 °C		61.9	64.6	60.7	27.2	-1.5	1,7
3CoO.Fe <sub>2</sub> O <sub>3</sub> .SiO <sub>2</sub> Composition 3 1100 °C		53.6	58.3	54.0	24.4	-2.5	1.4

### Pigment deposition and pigmentation performance

The implementation of the pigments in glazes is accompanied by color saturation lose, and the corresponding glazes possess more neutral colors, compared with those of the pigments used. The colors of ceramic tiles were determined after 5% additions of pigments, calcined at 1100 °C to kaolin doped glazes and subsequent deposition. The results are shown in Table 4.

As expected, the colors of the obtained glazes were more pale and neutral than those of the pigments used. In order to quantify the color changes coinciding the application of the investigated pigments in glaze compositions, a new criterion, named “Color Intensity Lose Rate” (CILR%) was used. Its values were calculated, using a simple equation (Eq. (1)), in order to determine the changes of the color parameters, according to CIE-L-a-b system:

$$\text{CILR} = \frac{(P_{cp} - G_{cp})}{P_{cp}} \times 100 \quad (1)$$

where  $P_{cp}$  and  $G_{cp}$  mean pigment and glaze color parameters and the subscribe index “cp” means the respective color parameter, according to CIE-L-a-b system.

The colors of the obtained tiles were similar to those of the pigments used, exhibiting high pigment stability in the glaze melt at 1145 °C. As expected, the glazes were paler, due to the relatively low pigment content. Indeed, when the values from Tables 3 and 4 in all cases, the CILR of the luminosity ( $L^*$ ) increases with 36.30% for composition 1; 15.19% for composition 2, and 129.50% for composition 3. According to parameter  $a^*$ , both compositions 1, and 2 have reddish appearance, whereas composition 3 is rather greenish, possessing negative  $a^*$  values. The respective glazes are relatively more colorless than the corresponding pigments. The CILR values of  $a^*$  parameter decrease with 37.21% for the first composition, whereas for the latter compositions the color intensity decay is 48.96% and 52.00% for compositions 2 and 3, respectively. The blue/yellow parameter reveals that all the pigments are yellowish, possessing positive  $b^*$  values. The corresponding glazes are with more neutral colors, compared to the pigments used. Thus, the  $b^*$  parameter decreases with 50.00%

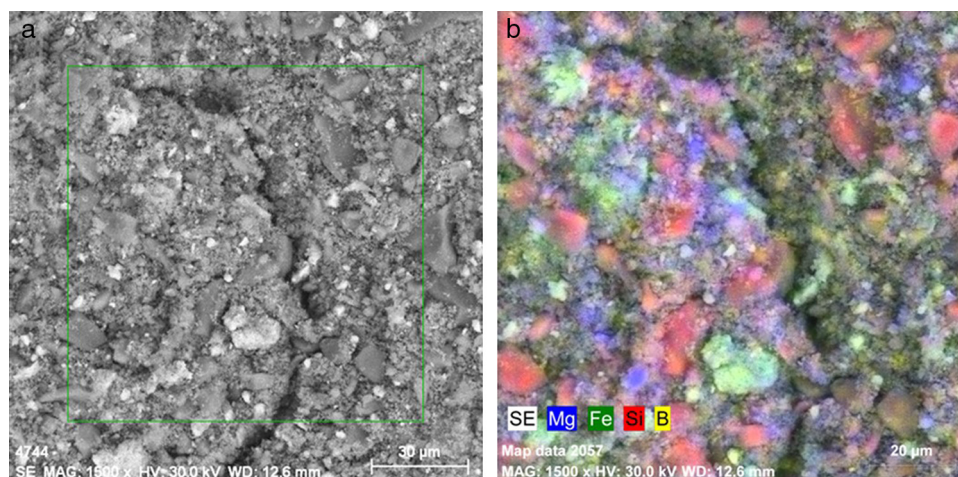


Fig. 11 – SEM images and EDX map analyses of the investigated pigments sintered at 1100 °C.

Table 4 – CIE-L-a-b colorimetric parameters of the glazed tiles.

Sample	Color	R	G	B	L*	a*	b*
5% Comp. 1 - 1100°C 95% glaze		162	153	152	64.2	2.7	1.6
5% Comp. 2 - 1100°C 95% glaze		222	185	164	78.1	9.8	16.1
5% Comp. 3 - 1100°C 95% glaze		133	135	132	56	-1.2	0.5

for composition 1; 59.55% for composition 2, and 64.28% for the third composition, respectively. As can be seen, the most remarkable differences among the color saturation lose, after deposition belong to the  $L^*$  parameter. It almost does not change in the case of the Ca-containing composition, whereas the cobalt pigment becomes more than twice lighter, converting from almost black to pale gray colored glaze with greenish shade. In contrary, the blue color component saturation decrement is rather similar for all the compositions, with insignificant CILR variance of only 14% among the samples, although the occurrence of cobalt in the third composition. The second composition converts its color from maroon pigment to “rose dust” glaze.

## Conclusions

Reddish brown and gray ceramic pigments were synthesized from Ca, Mg, and Co doped  $\text{Fe}_2\text{O}_3\text{-SiO}_2$  system by the solid state calcination method. The optimal results were registered for the samples calcination at 1100 °C.

The XRD analysis results have evinced occurrence of andradite, wollastonite, hematite and cristobalite for  $3\text{CaO}\cdot\text{Fe}_2\text{O}_3\cdot 3\text{SiO}_2$  based pigments. For composition  $3\text{MgO}\cdot\text{Fe}_2\text{O}_3\cdot\text{SiO}_2$ , the XRD spectra showed presence of magnesoferrite, forsterite, hematite and cristobalite and the pigments calcination from the  $3\text{CoO}\cdot\text{Fe}_2\text{O}_3\cdot\text{SiO}_2$  system were composed by  $\text{CoFe}_2\text{O}_4$ ,  $\text{Co}_2\text{SiO}_4$  and cristobalite. Furthermore, the calcination temperature elevation led to altering of

the pigments compositions by increase of the andradite, magnesoferrite, and  $\text{CoFe}_2\text{O}_4$  phase content.

The EPR spectra for composition 2 (i.e.  $3\text{MgO}\cdot\text{Fe}_2\text{O}_3\cdot\text{SiO}_2$ ), can be attributed to occurrence of  $\text{Fe}_2\text{O}_3$  in supermagnetic state, evincing compositional and size distribution homogeneity of the nano-domains in the powder probe. Besides, magnetic exchange interactions between the  $\text{Co}^{2+}$  and  $\text{Fe}^{3+}$  ions in the  $\text{Fe}_{2.719}\text{O}_4\text{SiO}_{2.81}$  non-stoichiometric phase was registered for composition 3 (i.e.  $3\text{CoO}\cdot\text{Fe}_2\text{O}_3\cdot 3\text{SiO}_2$ ).

The Mössbauer spectra have indicated that the main iron fraction is included in hematite ( $\alpha\text{-Fe}_2\text{O}_3$ ), and lower Fe-fractions, involved in  $\text{MgFe}_2\text{O}_4$ , inverted spinel and the silicate matrix.

The color parameters quantification has revealed that all the pigments become darker with the calcination temperature elevation and the highest green segment value/-  $a^*$ /belongs to the pigment of composition 3, calcined at 1100 °C.

The SEM-EDX observations reveal coincidence of coarse particles with 10–20  $\mu\text{m}$  and shapeless smaller particles.

The implementation of the pigments in glazes is accompanied by color saturation lose, and the corresponding glazes possess more neutral colors, compared with these of the pigments used. In this sense, a new criterion is proposed for quantitative evaluation of the color changes caused by the application of the investigated pigments in glaze compositions. The most distinguishable variation belongs to the  $L^*$  parameter, because the first composition changes its brightness with only 15.19%, whereas the third composition becomes more that twice lighter after glazing. The second composition converts its color from maroon to “rose dust”.



The synthesized pigments in the present work can be successfully used for decoration layers of sanitary ceramic products.

## Acknowledgement

The present research is elaborated by the financial support of contract 2016-ΦP3-02 to the scientific research fund of “Angel Kanchev” University of Rousse (Bulgaria).

The contribution of KAI Group-Khan Asparuh-JSC-(Bulgaria) is highly appreciated by the Authors.

## REFERENCES

- [1] R. Eppler, in: Kirk-Othmer (Ed.), *Encyclopedia of Chemical Technology*, John Wiley & Sons, 2013, <http://dx.doi.org/10.1002/0471238961.0315121505161612.a01.pub3>.
- [2] G. Monrós, in: Ronnier Luo (Ed.), *Pigment, Ceramic, Encyclopedia of Color Science and Technology*, Springer, 2014, ISBN 978-1-4419-8070-0. ON LINE ISBN 978-3-642-27851-8. <http://www.springerreference.com/docs/html/chapterdbid/348055.html>.
- [3] CPMA Classification and Chemical Description of the Complex Inorganic Color Pigments, Fourth Edition – January 2013 Update, Complex Inorganic Color Pigments Committee, Color Pigments Manufacturers Association, Inc., 2013.
- [4] C. Carter, M. Norton, *Ceramic Materials, Science and Engineering*, Springer, 2007.
- [5] R. Eppler, Selecting ceramic pigments, *J. Am. Ceram. Soc. Bull.* 66 (1987) 1600–1610.
- [6] F.J. Torres, M.A. Tena, J. Alarcon, Rietveld refinement study of vanadium distribution in V<sup>4+</sup>-ZrSiO<sub>4</sub> solid solutions obtained from gels, *J. Eur. Ceram. Soc.* 22 (2002) 1991–1994.
- [7] J. Alarcon, Crystallization behaviour and microstructural development in ZrSiO<sub>4</sub> and V-ZrSiO<sub>4</sub> solid solutions from colloidal gels, *J. Eur. Ceram. Soc.* 20 (2000) 1749–1758.
- [8] M. Blosi, M. Dondi, S. Albonetti, G. Baldi, A. Barzanti, C. Zanelli, Microwave-assisted synthesis of Pr-ZrSiO<sub>4</sub>, V-ZrSiO<sub>4</sub> and Cr-YAlO<sub>3</sub> ceramic pigments, *J. Eur. Ceram. Soc.* 29 (14) (2009) 2951–2957.
- [9] F. Bondioli, F. Andreola, L. Barbieri, T. Manfredini, A. Ferrari, Effect of rice husk ash (RHA) in the synthesis of (Pr,Zr)SiO<sub>4</sub> ceramic pigment, *J. Eur. Ceram. Soc.* 27 (2007) 3483–3488.
- [10] G. Del Nero, G. Cappelletti, S. Ardizzone, P. Fermo, S. Gilardoni, Yellow Pr-zircon pigments: the role of praseodymium and of the mineralizer, *J. Eur. Ceram. Soc.* 24 (2004) 3603–3611.
- [11] R. Carter, Zircon-ceramic pigments, materials & equipment/whitewares, *Ceram. Eng. Sci. Proc.* 8 (11/12) (2009) 1156–1161.
- [12] M. Llusar, J. Badenes, J. Calbo, M. Tena, G. Monros, Environmental and colour optimisation of mineraliser addition in synthesis of iron zircon ceramic pigment, *Br. Ceram. Trans.* 99 (1) (2000) 14–22.
- [13] T. Dimitrov, L. Georgieva, S. Vassilev, Study of ceramic pigments from the ZrO<sub>2</sub>-SiO<sub>2</sub>-Fe<sub>2</sub>O<sub>3</sub> system, *Bol. Soc. Esp. Cerám. Vidrio* 42 (4) (2003) 235–237.
- [14] J. Alarcon, P. Escibamo, J. Gargallo, Cr-CaO-SiO<sub>2</sub> based ceramic pigments, *Br. Ceram. Trans. J.* 83 (3) (1984) 81–83.
- [15] J. Carda, G. Monros, P. Escibano, J. Alarcon, Synthesis of uvarovite Garnet, *J. Am. Ceram. Soc.* 72 (1989) 160–164.
- [16] V. Della, J. Junkes, C.R. Rambo, D. Hotzapf, Synthesis of the ceramic pigment victoria green (Ca<sub>3</sub>Cr<sub>2</sub>Si<sub>3</sub>O<sub>12</sub>) from CaCO<sub>3</sub>, Cr<sub>2</sub>O<sub>3</sub> and SiO<sub>2</sub>, *Quim. Nova* 31 (2008) 1004–1007.
- [17] R. Candeia, M. Bernardi, E. Longo, I. Santos, A. Souza, Synthesis and characterization of spinel pigment CaFe<sub>2</sub>O<sub>4</sub> obtained by the polymeric precursor method, *Mater. Lett.* 58 (2004) 569–572.
- [18] R. Candeia, M. Souza, M. Bernardi, S. Maestrelli, MgFe<sub>2</sub>O<sub>4</sub> pigment obtained at low temperature, *Mater. Res. Bull.* 41 (2006) 183–190.
- [19] N. Deraz, O. Abd-Elkader, Investigation of magnesium ferrite spinel solid solution with iron-rich composition, *Int. J. Electrochem. Sci.* 8 (2013) 9071–9081.
- [20] P. Medeiros, Y. Gomes, M. Bomio, I. Santos, M. Silva, Influence of variables on the synthesis of CoFe<sub>2</sub>O<sub>4</sub> pigment by the complex polymerization method, *J. Adv. Ceram.* 4 (2015) 135–141.
- [21] H. Yüngeris, E. Ozel, Effect of the milling process on the properties of CoFe<sub>2</sub>O<sub>4</sub> pigment, *Ceram. Int.* 39 (2013) 5503–5511.
- [22] M. Llusar, A. Forés, J.A. Badenes, J. Calbo, M.A. Tena, Guillermo Monrós, Colour analysis of some cobalt-based blue pigments, *J. Eur. Ceram. Soc.* 21 (8) (2001) 1121–1130.
- [23] T. Žák, Y. Jirásková, CONFIT: Mössbauer spectra fitting program, *Surf. Interface Anal.* 38 (2006) 710–714.
- [24] H.-S. Lee, B.-H. Lee, Synthesis of sphene (CaSnSiO<sub>5</sub>)-pink pigments with CrCl<sub>3</sub>, *J. Korean Ceram. Soc.* 46 (4) (2009) 405–412.
- [25] H.-Q. Li, M.-X. Chen, Q. Han, R.-X. Zhang, Effect of mineralizer on optical properties of yellow pigment of Sm<sub>0.3</sub>Ce<sub>0.66</sub>Mo<sub>0.04</sub>O<sup>(1.85+δ)</sup>, *Chin. Rare Earths* 35 (6) (2014) 62–66.
- [26] H. Zhang, J. Wang, L. Wang, J. Du, The research of mineralizers of the silicon-chrome-green pigment, *Adv. Mater. Res.* 750–752 (2013) 1746–1749.
- [27] A. Burkovíčová, Dohnalová F. Ž., P. Šulcová, Colour properties of pigments based on YMnO<sub>3</sub>, *Ceram. Mater.* 67 (1) (2015) 9–14.
- [28] H.S. Lee, B.H. Lee, The development of a chromium pink glaze coloring, *J. Ceram. Proc. Res.* 9 (3) (2008) 286–291.
- [29] K. Plataniotis, A. Venetsanopoulos, *Color Image Processing and Applications Engineering*, Monograph, Springer-Verlag, 2000, pp. 435.
- [30] P.E. López, J.B. Carda Castelló, E.C. Cordoncillo, *Esmaltes y pigmentos cerámicos*, Faenza Editrice Iberica s.l., Castellón, España, 2001, pp. 192–196, ISBN 84-87683-19-3.